Inorganic Chemistry

Article

pubs.acs.org/IC

New Family of Cerium Halide Based Materials: CeX_3·ROH Compounds Containing Planes, Chains, and Tetradecanuclear Rings

Shae Anne Vaughn,[†] Bryan C. Chakoumakos,[‡] Radu Custelcean,[§] Joanne O. Ramey,[∥] Mark D. Smith,[†] Lynn A. Boatner,*[,∥] and Hans-Conrad zur Loye*[,†]

[†]Department of Chemistry and Biochemistry, The University of South Carolina, Columbia, South Carolina 29208, United States

[‡]Quantum Condensed Matter Division, Oak Ridge National Laboratory, Oak Ridge, Tennessee 37831, United States

[§]Chemical Sciences Division, Oak Ridge National Laboratory, Oak Ridge, Tennessee 37831, United States

[∥]ORNL Center for Radiation Detection Materials and Systems, Materials Science and Technology Division, Oak Ridge National Laboratory, Oak Ridge, Tennessee 37831, United States

Supporting Information

ABSTRACT: Six members of a new family of cerium-halide-based materials with promising scintillation behavior have been synthesized in single crystal form, and their crystal structures were determined. Specifically, these new compounds are $[(CeCl_3)_7(BuOH)_{16}(H_2O)_2]\cdot(BuOH)_2$ (**1**), $(CeBr_3)_{14}(BuOH)_{36}$ (**2**), $[(CeCl_3)_7(1\text{-}PrOH)_{16}(H_2O)_2]\cdot(1\text{-}PrOH)_2$ (**3**), $[(CeBr_3)_7(1\text{-}PrOH)_{18}]\cdot(1\text{-}PrOH)_2$ (**4**), $[(CeCl_3)_6(iBuOH)_{15}]\cdot(iBuOH)_2$ (**5**), and $CeCl_3(sec\text{-}BuOH)_2(H_2O)$ (**6**). Additionally, the scintillation ability of compound **1** was established. The structures of these cerium-halide-based materials consist of catenated tetradecanuclear rings that arrange themselves into three distinct structural motifs which contain the largest lanthanide-based ring structures reported to date; the different motifs are obtained by involving specific alcohols during synthesis. Specifically, *n*-butanol and *n*-propanol lead to 1-D chains of tetradecanuclear rings, and *iso*-butanol leads to 2-D parquet-patterned sheets of rectangular tetradecanuclear rings, while *sec*-butanol results in a zigzag 1-D chain structure. One of the compounds, $[(CeCl_3)_6(iBuOH)_{15}]\cdot(iBuOH)_2$, has been shown to scintillate with a light yield of up to 1920 photons/MeV, and due to the presence of protons, it should be capable of detecting high energy neutrons without the necessity of prior thermalization. Furthermore, it also appears to be the first cerium-based compound that scintillates in spite of the fact that water coordinates to two of the Ce(III) centers within the structure.

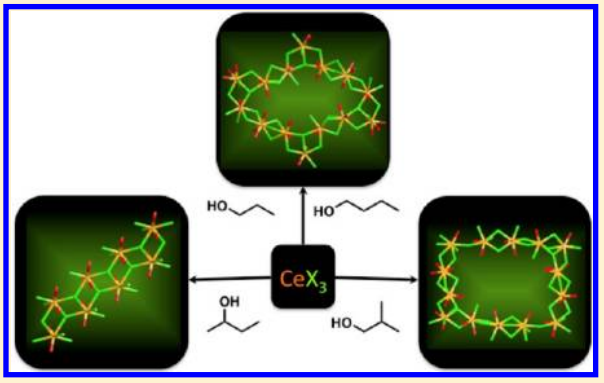

INTRODUCTION

It is known that high atomic number elements, such as cerium, have the ability to absorb high energy X-rays, γ-rays, and/or neutrons and that materials containing these elements can potentially function as efficient and sensitive scintillation materials.[1] Still, the discovery that cerium halide adducts not only are efficient scintillators, but also can be grown as large rare-earth metal−organic single crystals, has attracted significant interest in using this emerging family of materials for radiation detection.[1−4] As a class of new scintillator materials, these molecular adducts have proven to be highly effective for X-ray, γ-ray, and neutron detection.[4] Specifically, $CeCl_3(CH_3OH)_4$, the first material discovered in this class, demonstrated scintillation capabilities with surprising efficiencies, i.e., surpassing that of bismuth germanium oxide (BGO), a well-known scintillator.[1,2] Additionally, due to the presence of hydrogen in the compound, $CeCl_3(CH_3OH)_4$ is capable of detecting high-energy neutrons (e.g., 14.1 MeV neutrons from the deuterium-tritium reaction) without the necessity of employing prior thermalization.[4] This capability is not present in the case of the inorganic cerium activated inorganic halides such as $LaBr_3$:Ce or $LaCl_3$:Ce.[5−8]

The syntheses of other scintillators with compositions related to that of $CeCl_3(CH_3OH)_4$, such as $CeBr_3(CH_3OH)_4$, followed rapidly, thereby expanding the family of scintillation materials into the bromide derivatives.[9,10] These efficient molecular adduct scintillators represent only the first examples of an entire family of cerium-containing inorganic−organic hybrid materials that can be synthesized and grown as single-crystals with promising scintillation capabilities.

Here we report on the synthesis and structural characterization of the next generation of potential cerium-based metal−organic scintillators as represented by the following six compounds: (1) $[(CeCl_3)_7(BuOH)_{16}(H_2O)_2]\cdot(BuOH)_2$, (2) $(CeBr_3)_{14}(BuOH)_{36}$, (3) $[(CeCl_3)_7(1\text{-}PrOH)_{16}(H_2O)_2]\cdot(1\text{-}$

Received: February 14, 2012

   dx.doi.org/10.1021/ic3003349 | Inorg. Chem. XXXX, XXX, XXX−XXX

PrOH)$_2$, (4) [(CeBr$_3$)$_7$(1-PrOH)$_{18}$]·(1-PrOH)$_2$, (5) [(CeCl$_3$)$_6$(iBuOH)$_{15}$]·(iBuOH)$_3$, (6) CeCl$_3$(*sec*-BuOH)$_2$(H$_2$O).

All of these compounds belong to a class of extended structures containing catenated rings (see Figure 1). Note that, for the sake of simplicity and brevity, in the future we will adopt a nomenclature in which the six compounds listed above are referred to by their associated number.

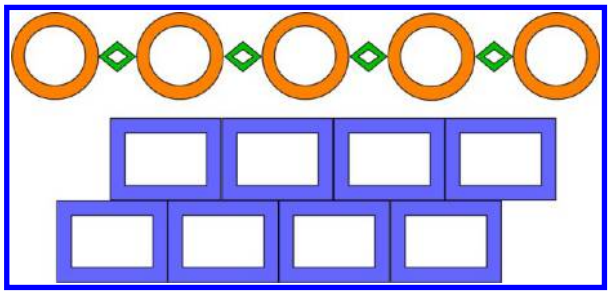

Figure 1. Schematic representation of coordination motifs where orange circles represent the tetradecanuclear rings linked via halide bridges (shown in green) found in compounds **1**–**4**, while blue rectangles represent the tetradecanuclear rings found in compound **5**.

The general synthetic approach for forming the subject six compounds is based on the fact that dimeric adducts of lanthanide halides can be achieved through the coordination of small ligands such as methanol, THF, and isopropanol. It has also been shown in the literature that these materials can easily form 1-D chains upon the incorporation of water into the structure.[11−15] Loiseau et al. have observed similar trends with NdCl$_3$ and EuCl$_3$ incorporating much larger ligands such as phenanthroline and terpyridine.[16,17]

General Procedure for the Preparation of Compounds 1−6. CeCl$_3$ (99.99%) was purchased from Sigma Aldrich, and CeBr$_3$ (99.9%) was purchased from Strem Chemicals; both were packed under argon and stored in a glovebox. Anhydrous butanol (99.4%) was purchased from Acros, and anhydrous 1-propanol (99.5%) was purchased from Sigma-Aldrich. All of the anhydrous solvents were received with septa seals.

The as-supplied CeCl$_3$ is placed in a quartz tube where it is heated under vacuum and melted, and then the molten salt is filtered through a quartz frit filter into a pointed Bridgman crucible. The Bridgman ampule is then sealed with a hydrogen oxygen torch and lowered through a vertical Bridgman furnace. Following the Bridgman growth cycle, the ampule is opened in a drybox and 30 g of the resulting material is placed in a beaker with 100 mL of the desired solvent (e.g., butanol, propanol, etc.). As these materials are highly hygroscopic the incorporation of small amounts of water despite the precautions undertaken to prevent water interactions can nonetheless occur, as seen in the case of compounds **1**, **3**, and **6**.

The as-supplied CeBr$_3$, approximately 0.50 g, is placed in a round-bottom flask and septa sealed inside a drybox. After removal from the drybox, approximately 10 mL of anhydrous alcohol was transferred via a nitrogen-purged syringe into the flask to create a saturated solution in which some of the salt remains as a precipitate. The solution is then syringe-filtered into a nitrogen-purged glass vessel and allowed to slowly evaporate in a nitrogen atmosphere, leading to the formation of single crystals in approximately 75% yield based on visual observations of crystals formed and the remaining cerium salt starting material remaining, as nearly all of the solvent evaporates during crystallization.

Scintillation Studies. The light yield was measured by placing the sample on the face of a photomultiplier tube (Burle 8850) with an intervening optical coupling fluid. Four layers of Teflon tape were then applied over the top of the crystal to enhance the light collection efficiency, and a shaping time of 0.5 μs was used in obtaining the pulse height spectrum. During the data collection process, an aluminum chamber containing a desiccant was sealed onto the face of the photomultiplier tube using an "O" ring to protect the crystal from exposure to the atmosphere.

Luminescence Studies. Compound **2** was excited at approximately 360 nm using a Leica M216F fluorescent stereomicroscope to obtain an optical image of the luminescence of a plate crystal located in the glass crystallization vessel, which is septa sealed and filled with nitrogen to prevent degradation of the crystal, as these materials are air sensitive. Therefore, the image was captured through the glass of the vial. In order to acquire the luminescence spectra of compound **2**, a polycrystalline powder was obtained through the evaporation of a supersaturated solution of CeBr$_3$ and *n*-butanol, the same method used to grow single crystals of compound **2**. Attempts to obtain PXRD patterns were made; however, due to the hygroscopic nature of the material, these were unsuccessful. The polycrystalline powder of **2** was excited at 232 nm, using a LS 55 spectrofluorometer, and exhibited a broad emission ranging from 378 nm out to 445 nm using a 1% attenuator filter to obtain the spectra. The emission maxima were observed at 378 and 402 nm, respectively. The polycrystalline powder was sealed with grease between quartz plates under a nitrogen atmosphere to prevent degradation of the material. To eliminate the possibility that the observed emission is due to unreacted CeBr$_3$ starting material, luminescence data were also collected of the starting material for comparison.

Crystallographic Studies. The structures were solved by single-crystal XRD; X-ray intensity data from single crystals of compounds **2** and **4** were measured at 100(2) K, and those for compounds **1**, **3**, **5**, and **6** were measured at 173(2) K using a Bruker SMART APEX diffractometer (Mo Kα radiation, λ = 0.710 73 Å). Raw area-detector data frame processing was performed with the SAINT+ and SADABS programs.[18] Final unit cell parameters were determined by least-squares refinements of large sets of reflections taken from each data set. Direct methods of structure solution, difference Fourier calculations, and full-matrix least-squares refinement against F^2 were performed with SHELXTL.[19] For compounds **2**, **3**, **4**, and **6**, hydrogen atoms bonded to carbon were placed in geometrically idealized positions and included as riding atoms.

Due to disorder among the ligands of compounds **4** and **5**, i.e., the hydrophobic ends of some of the butanol and propanol groups, the formulas presented are calculated on the basis of the crystal structure and evidence from the other analogous compounds presented herein; disorder-modeling details can be found in the Supporting Information. The crystal data and structure refinement results are summarized in Table 1.

RESULTS AND DISCUSSION

Our exploration of cerium-halide-based compounds has led to the synthesis of several new cerium-halide-containing materials exhibiting unique structural motifs that form via halide bridging between CeX$_n$ centers that are further modified via coordinated

dx.doi.org/10.1021/ic3003349 | Inorg. Chem. XXXX, XXX, XXX−XXX

Table 1. Crystal Data and Refinement for Compounds 1−6

	1	2	3	4	5	6
compd	$[(CeCl_3)_7(BuOH)_{16}(H_2O)_2]\cdot(BuOH)_2$	$(CeBr_3)_{14}(BuOH)_{36}$	$[(CeCl_3)_7(i\text{-}PrOH)_{16}\ (H_2O)_2]\cdot(i\text{-}PrOH)_2$	$[(CeBr_3)_7(i\text{-}PrOH)_{18}]\cdot(i\text{-}PrOH)_2$	$[(CeCl_3)_6(iBuOH)_{15}]\cdot(iBuOH)_3$	$CeCl_3(sec\text{-}BuOH)_2(H_2O)$
cryst syst	triclinic	triclinic	triclinic	triclinic	monoclinic	triclinic
space group	$P\bar{1}$	$P\bar{1}$	$P\bar{1}$	$P\bar{1}$	$P2(1)/n$	$P\bar{1}$
a/Å	14.2678(9)	22.2101(19)	13.6787(15)	13.5954(10)	18.0529(18)	5.7157(5)
b/Å	21.1043(13)	23.760(2)	20.156(2)	20.7910(15)	26.421(3)	11.3696(9)
c/Å	22.7005(14)	26.488(2)	21.192(2)	22.1835(15)	28.507(3)	13.3140(11)
α/deg	68.3360(10)	81.209(2)	104.428(2)	104.9620(10)	90.00	70.6260(10)
β/deg	81.2910(10)	89.414(2)	104.554(2)	105.1900(10)	104.334(2)	78.7400(10)
γ/deg	89.6730(10)	67.982(2)	97.692(2)	95.2610(10)	90.00	77.5950(10)
V/Å^3	6270.0(7)	12789(2)	5355.3(10)	5760.2(7)	13174(2)	789.91(11)
Z	2	2	2	1	4	2
T/K	173	100(2)	173	100(2)	173	173
$F(000)$	2710	6992	2746	3603	4888	406
D_{calcd} (Mg m^{-3})	1.541	1.996	1.749	2.206	1.319	1.735
μ/mm^{-1}	2.980	9.043	3.484	10.038	2.435	3.377
index ranges	$-19 \le h \le 19$	$-25 \le h \le 25$	$-18 \le h \le 18$	$-17 \le h \le 17$	$-24 \le h \le 24$	$-7 \le h \le 7$
	$-28 \le k \le 28$	$-27 \le k \le 27$	$-26 \le k \le 26$	$-26 \le k \le 26$	$-35 \le k \le 35$	$-14 \le k \le 15$
	$-30 \le l \le 30$	$-28 \le l \le 30$	$-28 \le l \le 28$	$-27 \le l \le 27$	$-38 \le l \le 37$	$-17 \le l \le 17$
R_{int}	0.0889	0.2155	0.0922	0.0906	0.1273	0.0240
data/restraints/ params	30 964/20/920	40 666/176/1684	26 487/3/855	23 827/72/869	32 580/3/643	3914/0/150
GOF on F^2	1.035	0.932	1.052	1.020	1.045	1.048
R1 = $[I > 2\sigma(I)]$	0.0543	0.0827	0.0600	0.0479	0.0783	0.0228
wR2 = $[I > 2\sigma(I)]$	0.1343	0.1611	0.1510	0.1077	0.2059	0.0588

dx.doi.org/10.1021/ic3003349 | Inorg. Chem. XXXX, XXX, XXX−XXX

alcohols, such as *n*-propanol, *n*-butanol, and isobutanol. The structures of the compounds denoted above as **1**−**4** consist of square antiprismatic, 8-coordinated Ce(III) cations that form tetradecanuclear rings through bridging halides, which also link the rings into infinite one-dimensional chains, and that, to the best of our knowledge, contain the largest lanthanide rings reported to date (Figure 2). While other large lanthanide ring structures are known in the literature, for example, the molecular decanuclear complexes $Dy_{10}(OC_2H_4OCH_3)_{30}$[20] and $[Y(OC_2H_4OMe)_3]_{10}$,[21] as well as the dodecanuclear complex $[Na(H_2O)_2]_4[Nd_{12}(\mu_3\text{-}OH)_{16}(EDTA)_8]^{8-}$,[22] the ring structures reported herein contain larger rings that, in addition, are catenated, thus representing a unique structural motif. Compound number **5** above exhibits a different structural motif wherein tetradecanuclear rings connect into a 2-D parquet pattern and exhibits a lamellar sheet structure, while compound **6** forms zigzag 1-D chains. Compounds **1**−**5** have channels along at least one crystallographic axis that are typically filled by alcohol molecules.

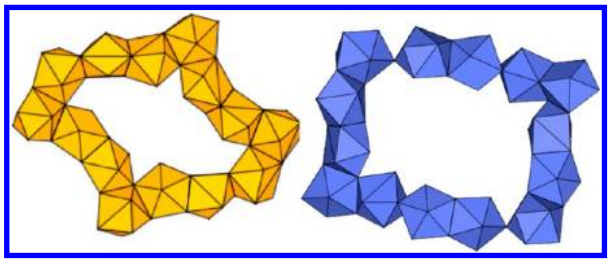

Figure 2. Edge-, face-, and corner-sharing polyhedra that make up the inorganic backbones of isostructural rings found in compounds **1**−**4** (left), and the rectangular rings found in compound **5** (right).

Structural Investigations. Compounds **1**−**4** share a common ring motif comprised of 14 Ce(III) cations bridged via halides through an intricate array of face- and edge-sharing polyhedra. Only the details of the ring structure of **1** are described, as it is representative of the connectivity observed in the ring structure of compounds **1**−**4**. Compound **1** is formed through halide bridging between seven distinct square antiprismatic polyhedra (Figure 3). Ce1 face-shares with Ce2 that acts as one of the four keystones of the tetradecanuclear ring. Ce2 edge-shares with both Ce1 and Ce3 through a μ_3-bridging bromide ligand; the ring propagates from Ce3 to Ce4 via face-sharing polyhedra. Ce4 edge-shares with Ce5, which, in turn, edge-shares with Ce6 the second keystone within the ring. Ce6 has a the same connectivity as Ce2, but it has a different coordination sphere due to the presence of three *n*-butanol ligands and two terminal chlorides, compared to two *n*-butanol ligands and three terminal chlorides for Ce2. Ce6 edge-shares to Ce7, which, in turn, face-shares to a symmetrically equivalent Ce1. Ce5 edge-shares with a symmetrically equivalent Ce5 of a neighboring ring, and thus propagates the 1-D chain of rings. Compounds **1**−**4** crystallize in the triclinic space group $P\bar{1}$, with identical 1-D chains of edge-shared rings. The stacking of the rings, however, is not the same for all four structures: **1**, **3**, and **4** exhibit AA stacking, while **2** exhibits AB stacking. When viewed along the [100] direction **1**, **3**, and **4** reveal an array of crystallographically observable 1-D channels (Figure 4). Compounds **1** and **3** exhibit 13 Å diameter rings, as measured from the outer edge of symmetrically equivalent chloride anions, while compound **4** has rings with an approximate diameter of 15 Å when measured from the outer edge of symmetrically equivalent bromide anions. Two uncoordinated butanol (**1**) and propanol (**3**, **4**) molecules reside in the center of the rings (Figure 5). Due to the extreme moisture sensitivity of these cerium halide structures, it has not been feasible to

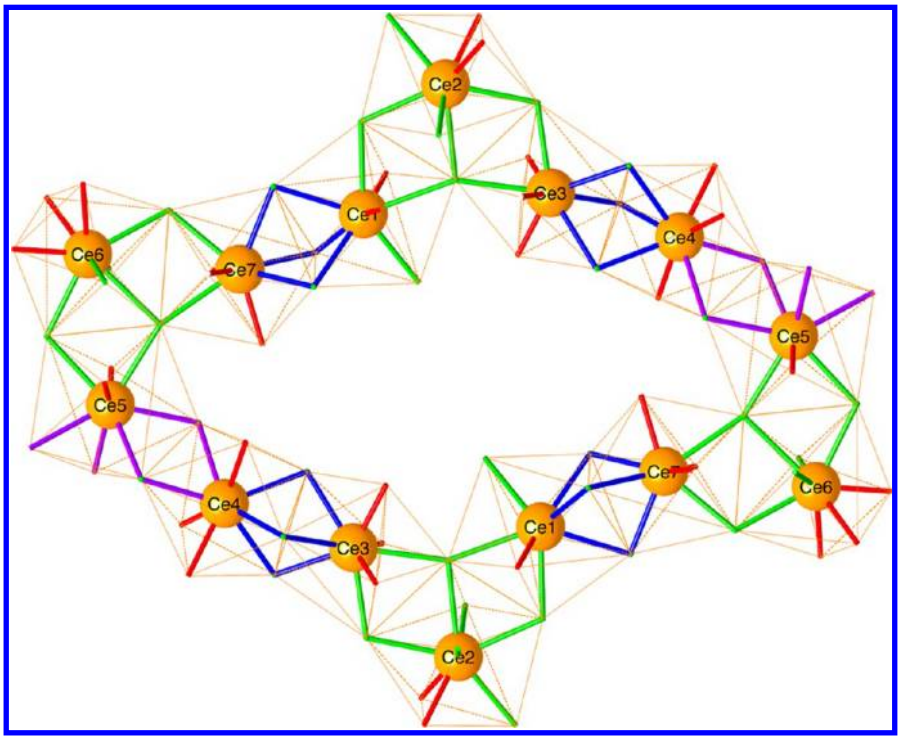

Figure 3. Connectivity of compound **1**, with edge-sharing μ_3-bridged polyhedra shown in green, bonds involved in edge-sharing shown in purple, and bonds involved in face-sharing shown in blue.

dx.doi.org/10.1021/ic3003349 | *Inorg. Chem.* XXXX, XXX, XXX−XXX

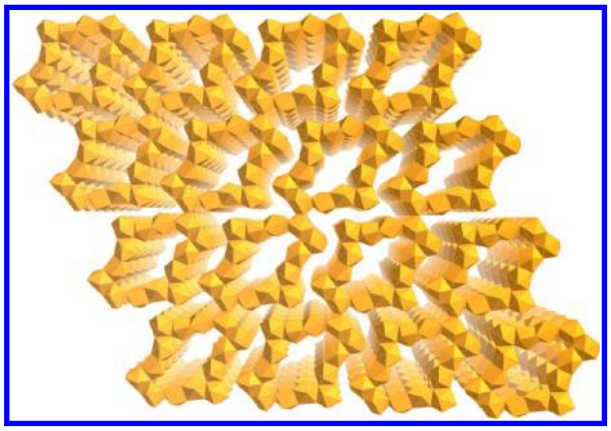

Figure 4. Compound **1**, channels formed by the inorganic polyhedra when viewed along the [100] direction (orange polyhedra represent the 8-coordinate Ce; BuOH ligands omitted for clarity).

explore the stability of the structures upon the removal of the guest ligands.

The interlayer spacing, approximately 14.0 Å in compound **1** and 11.6 Å in **3** and **4**, was determined by measuring the average distance from the Ce atoms in one chain to a lattice plane fit through the Ce atoms in a chain located above the first one. The difference in interlayer separation is expected since a shorter alkyl chain in compounds **3** and **4** creates a smaller hydrophobic region thereby leading to shorter interlayer spacing (Figure 6).

Compound **2** exhibits the same tetradecanuclear rings as **1**, **3**, and **4**. However, the layers in **2** are stacked in a staggered fashion, AB, in which the rings do not directly align, unlike those observed in compounds **1**, **3**, and **4**, which exhibit AA stacking (Figure 7). The interlayer distance of compound **2** was determined to be approximately 13.0 Å.

Compound **5** represents an intriguing structural deviation from **1**–**4**, since it forms a tetradecanuclear rectangular ring with edge-, face-, and corner-sharing polyhedra, rather than the previously observed circular ring with edge- and face-sharing only (Figure 8).

Compound **5** self-assembles into a parquet pattern in the form of slightly corrugated 2-D sheets that stack into a lamellar-type structure. The interlayer distance between Ce(III) cations in adjacent chains of compound **5** is approximately 13.2 Å (Figure 9), and the rings, as defined by the backbone structure, are approximately 9 × 15 $Å^2$. The structure has crystallographically observable rectangular channels (Figure 10).

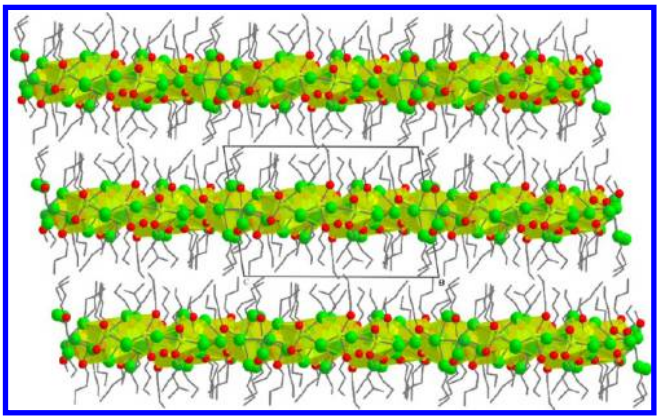

Figure 6. Layered structure of compound **1** when viewed down the *b*-axis (Ce = yellow, Cl = green, O = red, C–C bonds = black segments).

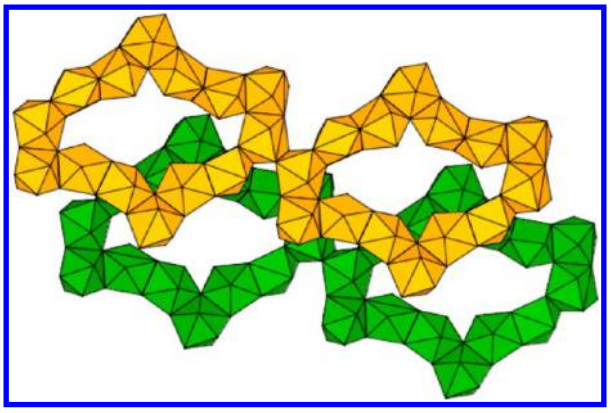

Figure 7. Edge-shared rings showing the staggered nature of the 1-D chains in compound **2**, with cerium polyhedra shown in green and orange.

The ring connectivity of compound **5** is quite complex as it forms a 2-D sheet structure. The connectivity of a single ring begins with Ce1, which face-shares with Ce2, which, in turn, edge-shares with Ce3 through a μ_3-bridging bromide ligand. Ce3 face-shares with Ce4 that leads to Ce5. Ce5 edge-shares with Ce4 and Ce6 through a μ_3-bridging bromide ligand; Ce6 is a polyhedron belonging to a neighboring ring and thus begins the connectivity of the 2-D structure. Continuing around the ring counter-clockwise leads back to Ce5, which corner-shares with a symmetrically equivalent Ce2 that edge-shares between Ce3 and Ce1 via a μ_3-bridging bromide ligand. Ce1 then edge-shares with Ce6. The connectivity of the sequence remains the

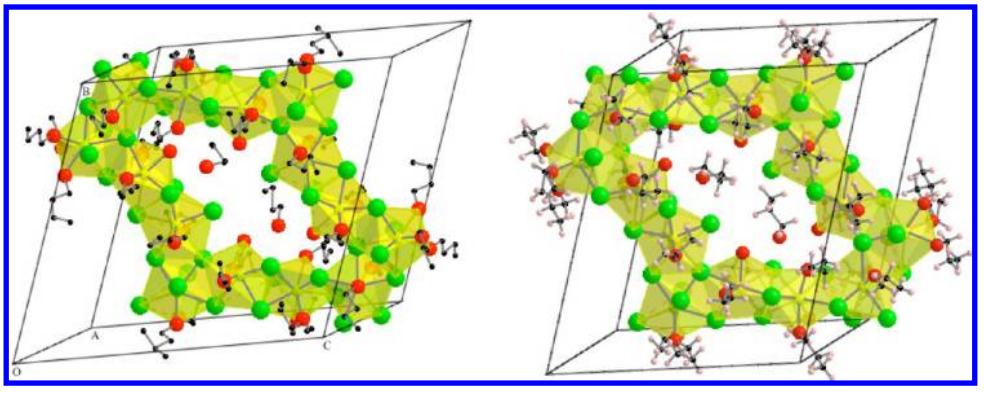

Figure 5. Molecular unit cells of compound **1** (left) and compound **2** (right). (Ce = yellow, Cl = green, O = red, C = black, H = white).

dx.doi.org/10.1021/ic3003349 | *Inorg. Chem.* XXXX, XXX, XXX–XXX

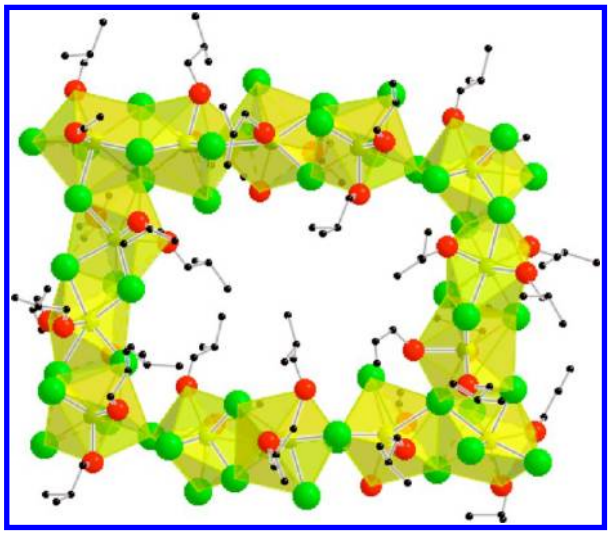

Figure 8. Isolated rectangular ring from compound **5** (Ce = yellow, Cl = green, O = red, C = black).

same; however, the order is then reversed, Ce1−Ce6−Ce5−Ce2−Ce3−Ce4−Ce5−Ce6−Ce1, moving counter-clockwise around the ring (Figure 11).

A simplified representation of compound **5** can be visualized as a series of zigzag chains that are bound together via corner-sharing polyhedra in order to create the sheet structure (Figure 12). The apparent cause for the intriguing structural uniqueness of **5** is the use of isobutanol as the structure-directing ligand in its synthesis.

Compound **6** forms a chain rather than a cyclic structure. The polyhedra of **6** are held together by three bridging chloride anions through edge-sharing polyhedra, resulting in a chain that adopts a zigzag pattern. It is likely that the racemic alcohol mixture plays a role in the structure formation, as both enantiomers of *sec*-butanol are observed in the crystal structure (Figure 13). Investigations into the structural outcome of using enantiomerically pure *sec*-butanol are underway, as this undoubtedly offers another way to control the topology of these materials. Average bond distances of the terminal, edge-, and face-sharing polyhedra are listed in Table 2. Further discussion of the structural analysis and thermal ellipsoid plots of compounds **1**−**6** can be found in the Supporting Information.

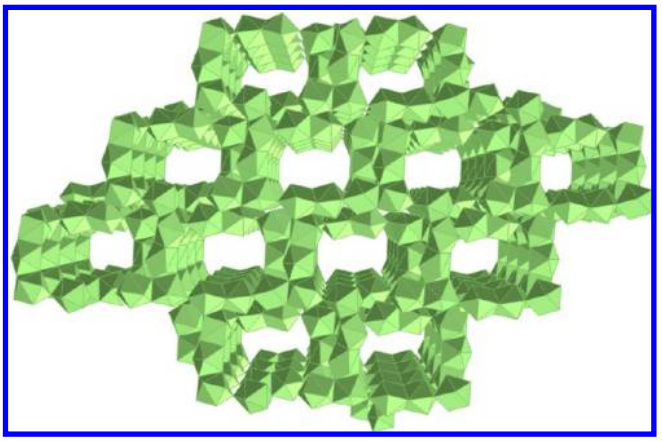

Figure 10. View of channels formed by the inorganic backbone of **5**, shown in light green. *sec*-BuOH ligands are omitted for clarity.

Among the compounds presented herein, the eight-coordination of the Ce cation occurs with four different ligand combinations, as enumerated in Table 3. Each cerium polyhedron is shared between two or three other cerium polyhedra via combinations of corner-, edge-, and face-sharing halogen bridges. Two of the ligand combinations offer multiple ways to join with adjacent polyhedra. Dihedral angles across the shared edges try to approach 180° to maintain low-energy configurations. The terminal halides participate in hydrogen bonding, e.g., between chains and between layers.

The packing of the hydrophobic alkyl chains of the various alcohols employed is believed to be an important driving force for the formation of these architectures. These chains show a propensity to segregate from the CeX_n polyhedra, thereby leading to the observed lamellar structures. Also, the bulk of the alkyl chains presumably play an important role in templating the various rings or chain motifs observed (Figure 14).

Scintillation Investigations. Scintillation measurements performed using a single crystal of compound **5** confirm the compound's ability to scintillate with a light yield of up to 1920 photons/MeV, making this new material not only a scintillator, but apparently also the first cerium-based compound that scintillates despite the fact that water coordinates to two of the Ce(III) centers within the structure. The extensive details of the scintillation characteristics and light yield using α-particle and γ-radiation will be presented elsewhere. The other compounds are expected to exhibit this property as well, and

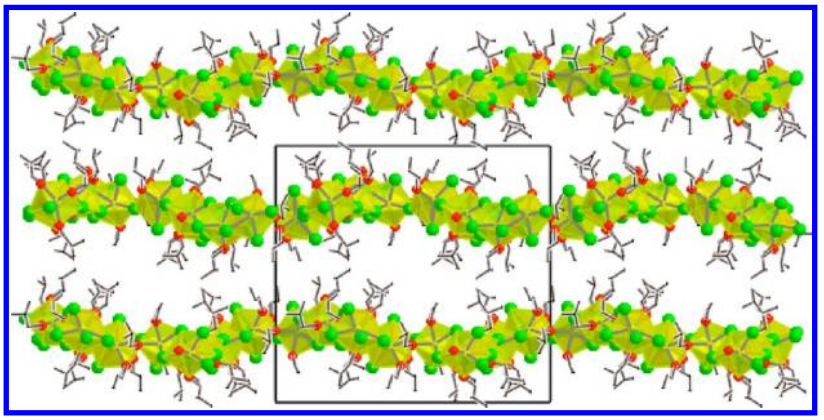

Figure 9. Lamellar structure of 2-D sheets found in compound **5** when viewed down the *b*-axis (Ce = yellow, Cl = green, O = red, C−C bonds = black segments).

dx.doi.org/10.1021/ic3003349 | *Inorg. Chem.* XXXX, XXX, XXX−XXX

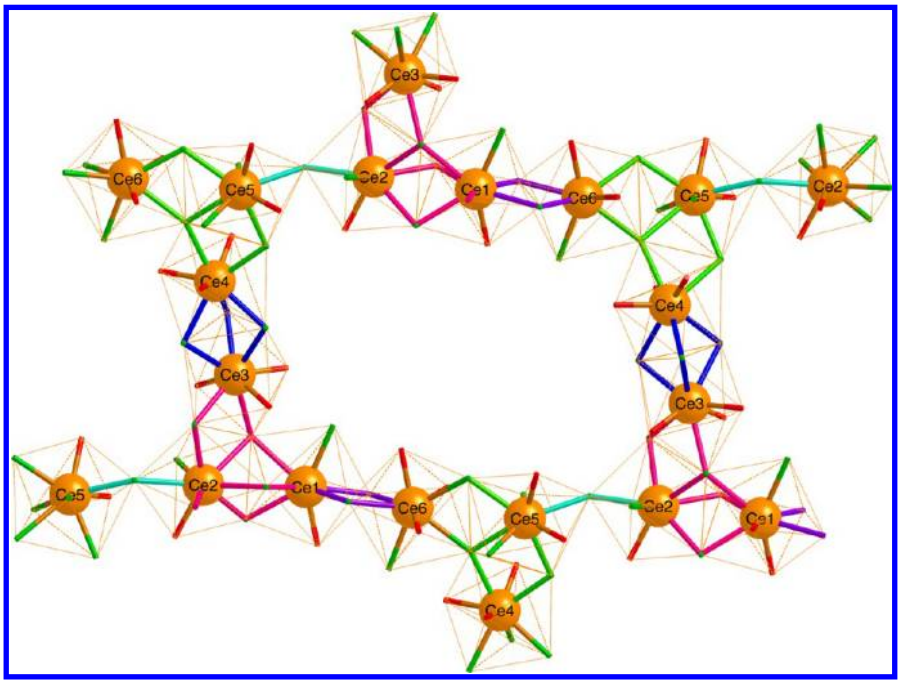

Figure 11. Connectivity of compound **5**, with face- and edge-sharing μ_3-bridged polyhedra shown in magenta, edge-sharing μ_3-bridged polyhedra shown in green, bonds involved in edge-sharing shown in purple, bonds involved in face-sharing shown in blue, and bonds involved in corner-sharing shown in aquamarine.

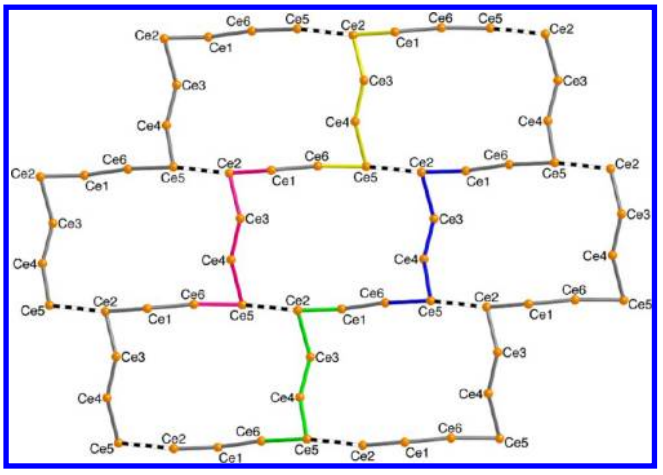

Figure 12. 2-D connectivity of Ce(III) cations of compound **5**, with only Ce atoms shown to simplify the structure. Symmetrically equivalent Ce(III) anions comprise one tetradecanuclear ring, shown in blue, yellow, pink, and green. Dashes between Ce2--Ce5 represent the corner-sharing polyhedra, which connect the 1D zigzag chains into a parquet patterned sheet structure.

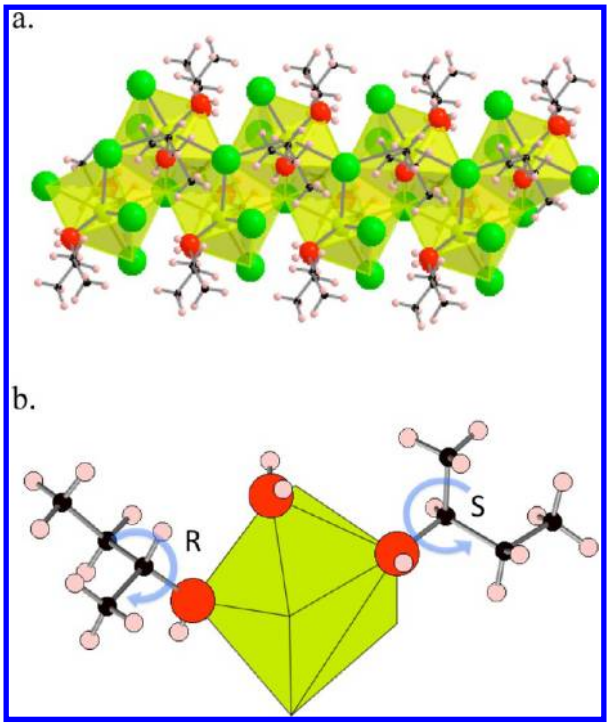

Figure 13. (a) Zigzag chain of **6**; Ce = yellow, Cl = green, O = red, C = black, and H = white. (b) Asymmetric unit of **6**, depicting the stereochemistry about the chiral carbon atoms of each *sec*-BuOH molecule.

efforts to obtain larger single crystals to determine the scintillation capabilities are underway. Potentially, these materials may also be applicable to catalysis and luminescence.[22−26]

Luminescence Investigations. Since materials that scintillate also luminesce, testing the luminescence of a potential scintillator is an excellent initial screening method. Hence, we have been screening our materials via luminescence measurements to determine whether or not to carry out more involved scintillation experiments. The luminescence study of compound **2** revealed that this material exhibits red-shifted luminescence as compared to $CeBr_3$, and exhibits two emission maxima at 378 and 402 nm, respectively, when excited at 360 nm (Figure 15). A stereomicroscope was used to obtain an optical image of the luminescence of a plate crystal of compound **2**. The image shows the expected violet-blue luminescence; an optical image of the crystal under ambient light is shown for comparison (Figure 15). Detailed measure-

dx.doi.org/10.1021/ic3003349 | *Inorg. Chem.* XXXX, XXX, XXX−XXX

Table 2. Table of Average Bond Lengths of the Terminal, Edge-, and Face-Sharing Halides for Compounds 1−6

	terminal	edge-sharing	face-sharing
1	2.834	2.894	2.863
2	2.967	3.065	3.034
3	2.819	2.910	2.876
4	2.981	3.065	3.032
5	2.819	2.899	2.893
6	2.777	3.016	n/a

Table 3. Types of Ce Coordination Polyhedra Observed with X = Halogen

shared edges	shared faces	shared corners	nonshared halogens
		$CeX_6(ROH)_2$	
1	1	0	1
2	0	0	3
2	0	1	2
3	0	0	0
		$CeX_5(ROH)_3$	
1	1	0	0
2	0	0	2
2	0	0	1
		$CeX_5(ROH)_2(H_2O)$	
1	1	0	0
		$CeX_6(ROH)(H_2O)$	
1	1	0	1

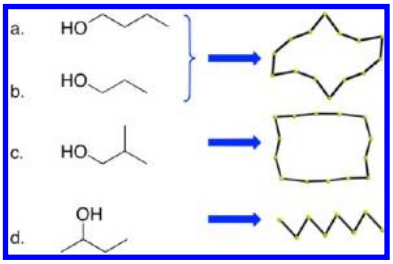

Figure 14. (a) BuOH, (b) 1-PrOH, (c) iBuOH, (d) *sec*-BuOH. Ligands **a** and **b** lead to the crystallization of tetradecanuclear rings, **c** leads to a rectangular tetradecanuclear ring, and **d** leads to a zigzag chain. Only Ce atoms are shown to highlight the shape of the ring or chain.

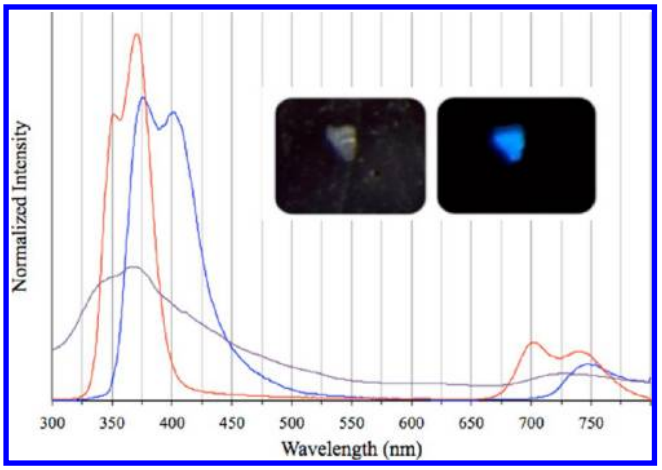

Figure 15. Clear plate crystal: optical picture on left, UV excited crystal on right. Luminescence emission spectra of **2** (blue), $CeBr_3$ (orange), and hydrated $CeBr_3$ (purple).

ments of the scintillation properties of the different structural analogues will be carried out in the near future.

CONCLUSIONS

Six members of a new family of cerium-halide-based materials, $[(CeCl_3)_7(BuOH)_{16}(H_2O)_2]\cdot(BuOH)_2$ (**1**), $(CeBr_3)_{14}(BuOH)_{36}$ (**2**), $[(CeCl_3)_7(1\text{-}PrOH)_{16}(H_2O)_2]\cdot(1\text{-}PrOH)_2$(**3**), $[(CeBr_3)_7(1\text{-}PrOH)_{18}]\cdot(1\text{-}PrOH)_2$ (**4**), $[(CeCl_3)_6(iBuOH)_{15}]\cdot(iBuOH)_2$ (**5**), and $CeCl_3(sec\text{-}BuOH)_2(H_2O)$ (**6**), with promising scintillation behavior have been synthesized and structurally characterized. The formation of rings containing 14 Ce(III) cations as vertices has occurred in four different systems, **1**−**4**, suggesting that this ring-structure arrangement is particularly stable under the synthesis conditions used here and indicating that additional members of this family of scintillator materials can likely be prepared using different alcohol adducts. Interestingly, ligands with bulkier substituents have led to 2-D parquet patterned sheets composed of tetradecanuclear Ce(III)-containing rectangular rings. Considering the wide variety of structural motifs prepared so far, it is likely that additional motifs can be stabilized using modified synthetic conditions. It is likely that further investigations of this family of materials will lead to better control of their topology and, potentially, of their ability to scintillate with higher efficiencies and environmental robustness.

ASSOCIATED CONTENT

Supporting Information

CIF data and additional figures and in depth refinement details. Further discussion of the luminescence. This material is available free of charge via the Internet at http://pubs.acs.org.

AUTHOR INFORMATION

Corresponding Author

*E-mail boatnerla@ornl.gov (L.A.B.), zurloye@mailbox.sc.edu (H.-C.z.L.).

Notes

The authors declare no competing financial interest.

ACKNOWLEDGMENTS

Research at the Oak Ridge National Laboratory was sponsored in part by the Materials Sciences and Engineering Division (L.A.B.), the Division of Chemical Sciences, Geosciences, and Biosciences (R.C.), and the Scientific User Facilities Division (B.C.C.), Office of Basic Energy Sciences, U.S. Department of Energy. Financial support from the National Science Foundation through Grant CHE-0714439 is gratefully acknowledged.

REFERENCES

(1) Boatner, L. A.; Wisniewski, D.; Neal, J. S.; Ramey, J. O.; Kolopus, J. A.; Chakoumakos, B. C.; Wisniewska, M.; Custelcean, R. *Appl. Phys. Lett.* **2008**, *93*, 244104/1−244104/3. Doty, F. P.; Bauer, C. A.; Skulan, A. J.; Grant, P. G.; Allendorf, M. D. *Adv. Mater. (Weinheim, Ger.)* **2009**, *21*, 95−101.

(2) Boatner, L. A.; Wisniewski, D. J.; Neal, J. S.; Bell, Z. W.; Ramey, J. O.; Kolopus, J. A.; Chakoumakos, B. C.; Custelcean, R.; Wisniewska, M.; Pena, K. E. *Proc. SPIE* **2009**, *7449*, 74491E/1−74491E/12.

(3) Chakoumakos, B. C.; Custelcean, R.; Ramey, J. O.; Kolopus, J. A.; Jin, R.; Neal, J. S.; Wisniewski, D. J.; Boatner, L. A. *Cryst. Growth Des.* **2008**, *8*, 2070−2072.

dx.doi.org/10.1021/ic3003349 | *Inorg. Chem.* XXXX, XXX, XXX−XXX

(4) Neal, J. S.; Boatner, L. A.; Bell, Z. W.; McConchie, S. M.; Wisniewski, D.; Ramey, J. O.; Kolopus, J. A.; Chakoumakos, B. C.; Wisniewska, M.; Custelcean, R. *IEEE Trans. Nucl. Sci.* **2010**, *57*, 1692−1695.
(5) Shah, K. S.; Glodo, J.; Higgins, W.; van Loef, E. V. D.; Edgar, V. D.; Moses, W. W.; Derenzo, S. E.; Weber, M. J. *IEEE Trans. Nucl. Sci.* **2005**, *52*, 3157−3159.
(6) Higgins, W. M.; Churilov, A.; van Loef, E. V.; Glodo, J.; Squillante, M.; Shah, K. J. *Cryst. Growth* **2008**, *310*, 2085−2089.
(7) Guss, P.; Reed, M.; Yuan, D.; Reed, A.; Mukhopadhyay, S. *Nucl. Instrum. Methods Phys. Res., Sect. A* **2009**, *608*, 297−304.
(8) Matson, D. W.; Graff, G. L.; Male, J. L.; Johnson, B. R.; Nie, Z.; Joly, A. G.; Olsen, L. C. *Thin Solid Films* **2010**, *518*, 3194−3198.
(9) van Loef, E. V.; Glodo, J.; Higgins, W. M.; Shah, K. S. *IEEE Nucl. Sci. Symp. Conf. Rec.* **2009**, 1415−1416.
(10) Vaughn, S. A.; Severance, R. C.; Smith, M. D.; zur Loye, H.-C.. *Cryst. Growth Des.* **2011**, *11*, 5072−5078.
(11) Boyle, T. J.; Ottley, L. A. M.; Alam, T. M.; Rodriguez, M. A.; Yang, P.; McIntyre, S. K. *Polyhedron* **2010**, *29*, 1784−1795.
(12) Evans, W. J.; Feldman, J. D.; Ziller, J. W. *J. Am. Chem. Soc.* **1996**, *118*, 4581−4584.
(13) Barnhart, D. M.; Frankcom, T. M.; Gordon, P. L.; Sauer, N. N.; Thompson, J. A.; Watkin, J. G. *Inorg. Chem.* **1995**, *34*, 4862−4867.
(14) Willey, G. R.; Woodman, T. J.; Drew, M. G. B. *Polyhedron* **1997**, *16*, 3385−3393.
(15) Chakoumakos, B. C.; Custelcean, R.; Ramey, J. O.; Boatner, L. A. *Inorg. Chim. Acta* **2012**, *384*, 23−28.
(16) Lhoste, J.; Perez-Campos, A.; Henry, N.; Loiseau, T.; Rabu, P.; Abraham, F. *Dalton Trans.* **2011**, *40*, 9136−9144.
(17) Lhoste, J.; Henry, N.; Loiseau, T.; Abraham, F. *Inorg. Chem. Commun.* **2011**, *14*, 1525−1527.
(18) *SMART Version 5.630, SAINT+ Version 6.45 and SADABS Version 2.10*; Bruker Analytical X-ray Systems, Inc.: Madison, WI, 2003.
(19) Sheldrick, G. M. *Acta Crystallogr.* **2008**, *A64*, 112−122.
(20) Westin, L. G.; Kritikos, M.; Caneschi, A. *Chem. Commun.* **2003**, 1012−1013.
(21) Poncelet, O.; Hubert-Pfalzgraf, L. G.; Daran, J. C.; Astier, R. *J. Chem. Soc., Chem. Commun.* **1989**, 1846−1848.
(22) Zheng, Z. *Chem. Commun. (Cambridge, U.K.)* **2001**, 2521−2529.
(23) Mishra, S. *Coord. Chem. Rev.* **2008**, *252*, 1996−2025.
(24) Gunnlaugsson, T.; Stomeo, F. *Org. Biomol. Chem.* **2007**, *5*, 1999−2009.
(25) Albrecht, M. *Z. Anorg. Allg. Chem.* **2010**, *636*, 2198−2204.
(26) Piguet, C.; Buenzli, J.-C. G.; Bernardinelli, G.; Hopfgartner, G.; Williams, A. F. *J. Alloys Compd.* **1995**, *225*, 324−330.